

电润湿液体透镜暂态过程的测试与分析

徐荣青¹, 李雷¹, 孔梅梅^{1*}, 张宏超²¹南京邮电大学电子与光学工程学院, 江苏 南京 210023;²南京理工大学理学院, 江苏 南京 210094

摘要 提出在电压驱动下液体透镜的响应包括固有响应和强制响应,固有响应信号的函数形式由液体透镜的各种参数决定,与驱动电压无关,但其系数与驱动电压有关,强制响应与驱动电压具有相同的函数形式,液体透镜暂态过程的变化规律取决于固有响应,同样与驱动电压无关。因此,对同一液体透镜改变驱动电压仅改变暂态过程的响应幅度,不改变暂态过程的变化规律,从而也不改变液体透镜的响应时间。实验验证了液体透镜的响应可分解为固有响应和强制响应,测量了不同电压驱动下液体透镜的响应过程及响应时间,并对测试结果进行了理论分析。另外,观察到电润湿液体透镜的反冲现象,该现象出现在加载电压和撤去电压的初始阶段。

关键词 光学器件; 主动或自适应光学; 液体透镜; 暂态过程; 反冲现象

中图分类号 O436 文献标志码 A

DOI: 10.3788/AOS221899

1 引言

众多研究领域的兴起、发展均与新现象的发现密不可分,润湿这一研究领域起始于润湿现象,随着迟滞^[1-2]、接触角饱和^[3-5]等现象相继被发现,润湿理论及相关应用均得到了蓬勃发展^[6-9]。润湿的特性决定着应用,固定的润湿特性显然限制了其应用范围,而润湿性能的调控必然会拓展润湿的应用范围。调控润湿特性的方法主要有3种:一是在流体中添加纳米颗粒、表面活性剂等^[10-11];二是在固体表面加微结构^[12];三是外加物理场^[13]。在前两种方法中,润湿器件一旦制备完成,其润湿特性就确定了,而外加物理场的方法可实时控制润湿的性质,因而得到广泛应用。外加的物理场可以是电场、磁场、热场等,由于电场的产生与控制相对于其他场具有方便、简单、技术成熟等优势,因此电润湿理论与技术得到了优先发展^[14],而电润湿液体透镜是电润湿技术的一种典型应用^[15]。

目前国内外许多研究者已针对电润湿液体透镜的机理、性能及应用进行了大量深入的研究^[16-27],但由于透镜的多样性及问题的复杂性,电润湿的理论尚需完善,性能有待提高,新的应用有待开拓。从应用的角度出发,液体透镜的性能是关键,变焦透镜的两个主要性能指标是变焦后的焦距及变焦时间,而这两个性能指标取决于电润湿液体透镜的响应特性:响应经暂态过程至稳态,变焦后的焦距由稳态值决定,响应时间由暂

态过程决定。无论从理论还是从实验来看,对稳态响应的研究难度都远小于对暂态过程的研究,故目前电润湿液体透镜响应特性的研究主要集中在稳态响应^[28-29],对暂态过程的研究鲜见报道,对暂态过程还没有形成一个完全清晰统一的认识。

理论对实验有指导作用,但理论的建立需要以实验数据为基础,同时理论的正确性需要进一步的实验数据来验证,故理论与实验是相互促进的关系。目前,有关液体透镜暂态过程的实验数据非常有限。另外,客观存在的某种机制会以某些现象来展现,仔细观察这些现象有助于提示出新机制。可见,现象的发现在相关理论的建立、丰富和完善中起着重要作用,而这些现象能否被观察到取决于实验对象、测试方法及实验条件。目前电润湿机理依据的实验数据主要来源于采用高速摄影方法测试液滴的电润湿过程^[16,29-32]。高速摄影方法测量的时间精度取决于摄影的速度,需处理大量图像,不利于暂态过程的测试与分析。另外液滴作为实验对象,可控性差,在进行对比实验时,需要测量大量数据,耗时较长,而液滴在长时间内无法保持一致性,将会影响实验数据的可靠性。

本文提出电润湿液体透镜在电压驱动下的响应包括固有响应和强制响应,暂态过程的变化规律取决于固有响应,与驱动电压无关,且液体透镜的响应时间也与驱动电压无关。用自行研制的测试液体透镜响应过程的装置测试了不同电压驱动下液体透镜的响应过

收稿日期: 2022-10-31; 修回日期: 2022-12-07; 录用日期: 2022-12-19; 网络首发日期: 2023-01-06

基金项目: 国家自然科学基金青年科学基金(61905117)

通信作者: *kongmm@njupt.edu.cn

程,实验结果与提出的认识一致;发现电润湿液体透镜存在反冲现象。

2 暂态过程的描述

从理论上得到液体透镜的响应过程,涉及众多动力学参数,需要求解 Navier-Stokes 方程,这是具有自由界面的两相流问题。目前主要采用数值计算方法分析电润湿的过程,未见计算解析解的报道。清华大学的王飞等^[33]采用二阶投影法求解 Navier-Stokes 方程和 level set 函数,数值计算 MAC 网格,模拟了管道内液滴接触角的变化过程;南京邮电大学的赵瑞等^[34]采用 COMSOL 软件对液体透镜的响应过程进行数值仿真。尽管上述研究没有得到具体的解析解,但得到了相应的微分方程的解,其完全解包含通解和特解。通解的形式取决于特征方程的特征根,而特征根由液体透镜的各种参数决定,与液体透镜的驱动电压无关;通解的系数需要根据完全解的形式及初始条件确定,因此通解的系数与驱动电压有关。从响应的形式看,通解由系统的固有参数决定,与外界激励无关,称为固有响应,而特解的函数形式与外界激励的函数形式相同,称为强制响应;从响应的性质看,固有响应是暂态的,强制响应是稳态

的,故响应稳定前暂态过程的变化规律取决于固有响应。对于同一个液体透镜,在不同电压驱动下,固有响应函数的形式相同,驱动电压的变化仅改变固有响应函数,所以不同电压作用下,液体透镜暂态过程的变化规律相同,暂态过程持续的时间即响应时间相同。

3 暂态过程的测试与分析

3.1 实验装置

图 1 所示为自行研制的电润湿液体透镜响应过程的测试装置,该装置主要由氦氖激光器、电润湿液体透镜、光电探测器、函数发生器、高压放大器、示波器等组成。选用氦氖激光器作为光源是因为该类激光器的光束质量好、稳定性高、单色性强。光电探测器选用的是具有高灵敏度的光敏元器件,该器件可以克服波动和噪声的影响,区分出微弱细小的光信号,并把光信号转换成电信号。由于函数发生器的输出电压不足以驱动电润湿液体透镜,故需要使用高压放大器对此电压进行放大。数字示波器的主要功能是接收光电探测器输出的电信号,实时显示或记录光电探测器的输出电压随时间的变化关系。实验中使用的液体透镜是 ARCTIC 系列(Varioptic 公司)的 A-25H。

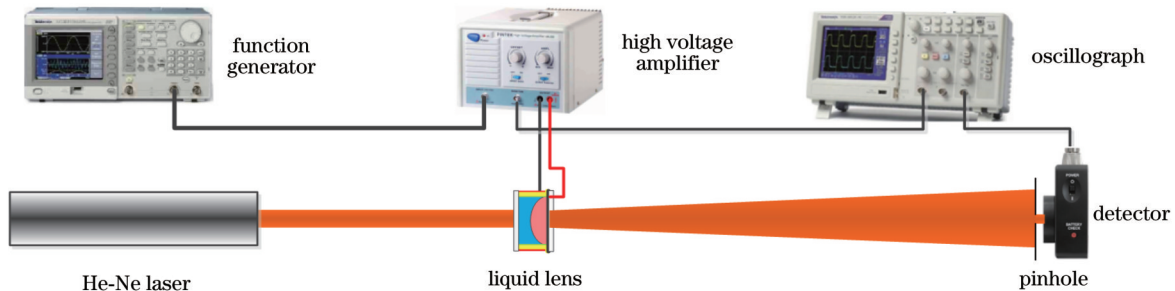


图 1 电润湿液体透镜响应过程的测试装置

Fig. 1 Experimental setup for measuring the response process of electrowetting liquid lens

当液体透镜的焦距在外加电压作用下发生变化(正负透镜状态)时,光电探测器所在位置的光强随之变化,且光电探测器输出的电压也随之变化^[35],因此探测器的输出电压与液体透镜的焦距有关,而液体透镜的焦距与液体透镜界面所处的状态有关,则测得的探测器输出电压随时间的变化过程不仅反映了液体透镜的变焦过程,也反映了液体透镜界面状态随时间的变化,即液体透镜的响应特性。

3.2 低频正弦信号驱动

为了验证液体透镜响应包含固有响应和强制响应,利用图 1 所示的装置测试了液体透镜在频率为 330 Hz、振幅为 23.2 V 的正弦信号驱动下的响应过程,并采用滤波方法对响应信号进行分析。

图 2(a)所示为驱动液体透镜的电压信号,插图为虚线方框区域在时间轴上的放大图;图 2(b)中实线表

示液体透镜的响应信号,点划线与虚线分别表示通过滤波方法分解得到的低通滤波信号与高通信号。电压作用在液体透镜上,通过产生电场力来驱动液体透镜界面变化,进而实现变焦,电场力 $F = \frac{\epsilon}{2d} U_d^2$,其中 U_d 为驱动电压, ϵ 为液体透镜介质层的介电常数, d 为介质层厚度。因此,液体透镜的驱动信号应是电场力,而不是施加的电压。图 2(c)中实线表示施加电压平方的时域信号,点划线表示图 2(b)虚线方框区域信号在时间轴上的放大。图 2(d)中实线和点划线分别表示图 2(c)中时域信号对应的频谱。由图 2(d)可知,施加电压的平方与响应信号高频滤波信号的频率均为 660 Hz;结合图 2(c)可知,高频滤波信号与施加电压平方的信号均为同频率的正弦信号,即响应信号的高通信号与驱动信号具有相同的函数形式,均为强制响应信号,而图 2(b)中点划线表示的低通滤波信号为固有

响应信号。可见,液体透镜的响应可分解为固有响应

和强制响应。

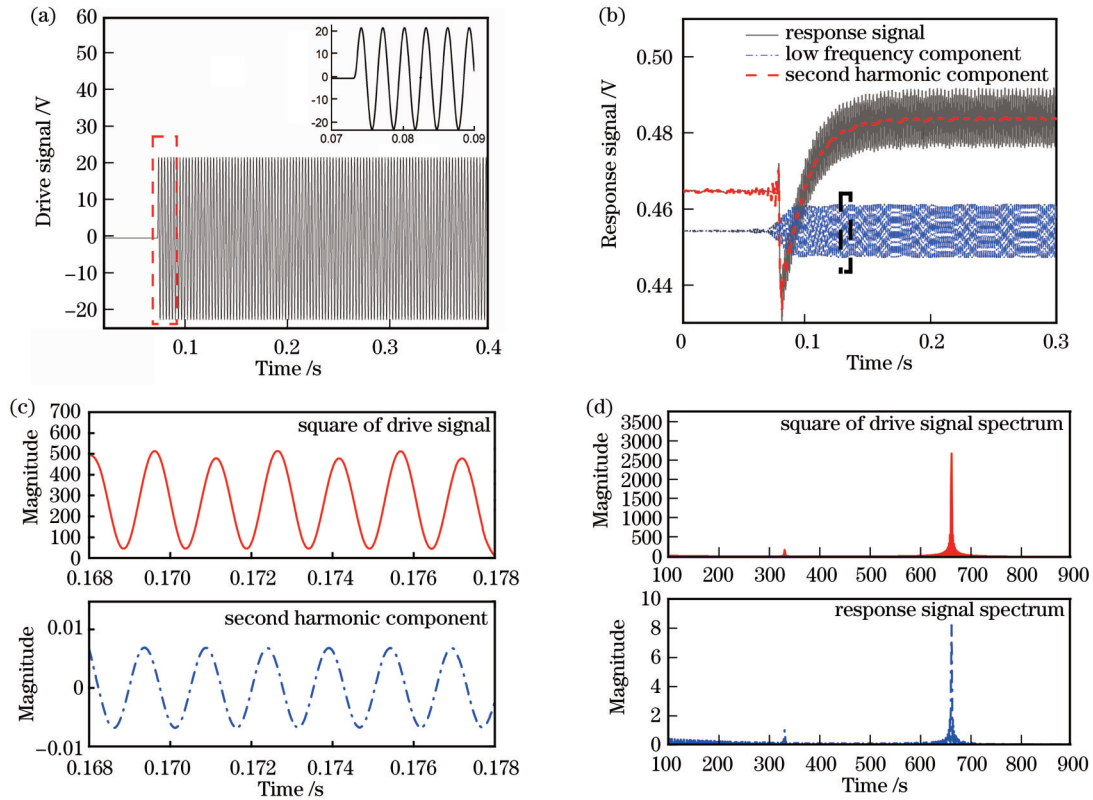


图 2 液体透镜在频率为 330 Hz、振幅为 23.2 V 的正弦信号驱动下的响应结果。(a)低频正弦驱动信号;(b)液体透镜的响应信号及其分解;(c)驱动电压的平方与响应信号高频滤波时域信号;(d)驱动电压的平方与响应信号高频滤波的频谱

Fig. 2 Response results of liquid lens driven by sinusoidal signal with frequency of 330 Hz and amplitude of 23.2 V. (a) Low frequency sinusoidal drive signal; (b) response signal of liquid lens and its decomposition; (c) square of driving voltage and time domain signal of high frequency filtering of response signal; (d) square of driving voltage and frequency spectrum of high frequency filtering of response signal

3.3 高频正弦信号驱动

为了进一步验证对于暂态过程认识的正确性,用图 1 所示的装置测试了液体透镜在不同幅度驱动电压作用下的响应特性。电润湿液体透镜由于要实现变焦功能,应用中需要在外界电压的作用下稳定在一个新焦距,可以施加直流电压或高频交流电压,交流驱动可减弱电荷累积效应,提高驱动效率,因此选用高频正弦交流信号。

图 3(a)所示为所使用的正弦交流驱动电压,该信号的振幅为 23.2 V,频率为 930 Hz,持续时间为 500 ms;图 3(b)所示为液体透镜在图 3(a)所示信号作用下的响应信号,其中 U_0 为没有驱动电压时光电探测器的输出电压值, U_s 为施加驱动电压且液体透镜稳定后光电探测器输出的电压, U_{m} 为加载电压时反冲信号的峰值, U_{m} 为撤去电压时反冲信号的峰值, ΔT_1 为从加载电压时刻到液体透镜从初始状态变化至加压后稳态时刻持续的时间,即加载响应时间, ΔT_2 为从撤去电压时刻到液体透镜从加压后的稳态变化至稳定的初始时刻持续的时间,即撤载响应时间。图 3(c)、(d)分别为图 3(b)中左侧实线方框和右侧虚线方框区域的

放大图。由图 3(c)和图 3(d)可知,无论是加载电压信号过程还是撤去电压信号过程,在液体透镜响应的初始阶段,液体透镜均是先向着目标状态快速变化,然后朝目标状态相反方向快速变化,且往相反方向的运动幅度较大,将这一现象称为反冲现象,这一阶段称为反冲阶段。随后液体透镜从反冲的峰值位置向目标稳态缓慢变化,这一阶段称为正常阶段。图 3(c)中的 Δt_1 和图 3(d)中的 Δt_2 分别为加载电压过程和撤载过程反冲阶段持续的时间。由图 3(b)可知,无论是加载还是撤载,液体透镜的响应暂态过程均存在反冲阶段和正常阶段,且反冲阶段的持续时间远小于正常阶段的持续时间。

图 4(a)所示为采用不同振幅正弦交流电压驱动下液体透镜的响应信号,驱动电压的频率及持续时间与图 3(a)相同。从图 4(a)可看出,在不同振幅的正弦电压作用下,液体透镜的响应信号仅是幅度不同,变化规律完全相同。图 4(b)、(c)分别为图 4(a)左侧实线方框和右侧虚线方框区域的放大图。在加载和撤载的初始阶段,液体透镜均是先向着目标状态快速变化,然后朝目标状态相反方向快速变化,且往相反方向的运

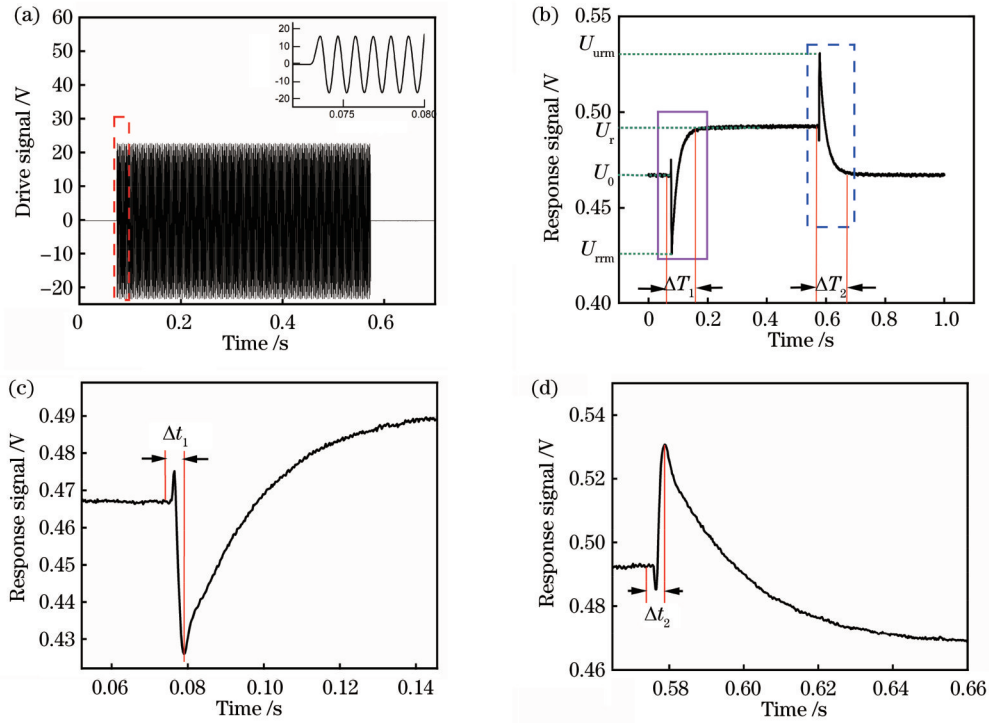


图 3 液体透镜在频率为 930 Hz、振幅为 23.2 V 的正弦信号驱动下的响应结果。(a) 高频正弦驱动信号；(b) 液体透镜的响应信号；(c) 加载电压瞬间液体透镜响应波形信号；(d) 撤去电压瞬间液体透镜响应波形信号
 Fig. 3 Response results of liquid lens driven by sinusoidal signal with frequency of 930 Hz and amplitude of 23.2 V. (a) High frequency sinusoidal driving signal; (b) response signal of liquid lens; (c) response waveform signal of liquid lens at the moment of loading voltage; (d) response waveform signal of liquid lens at the moment of removing voltage

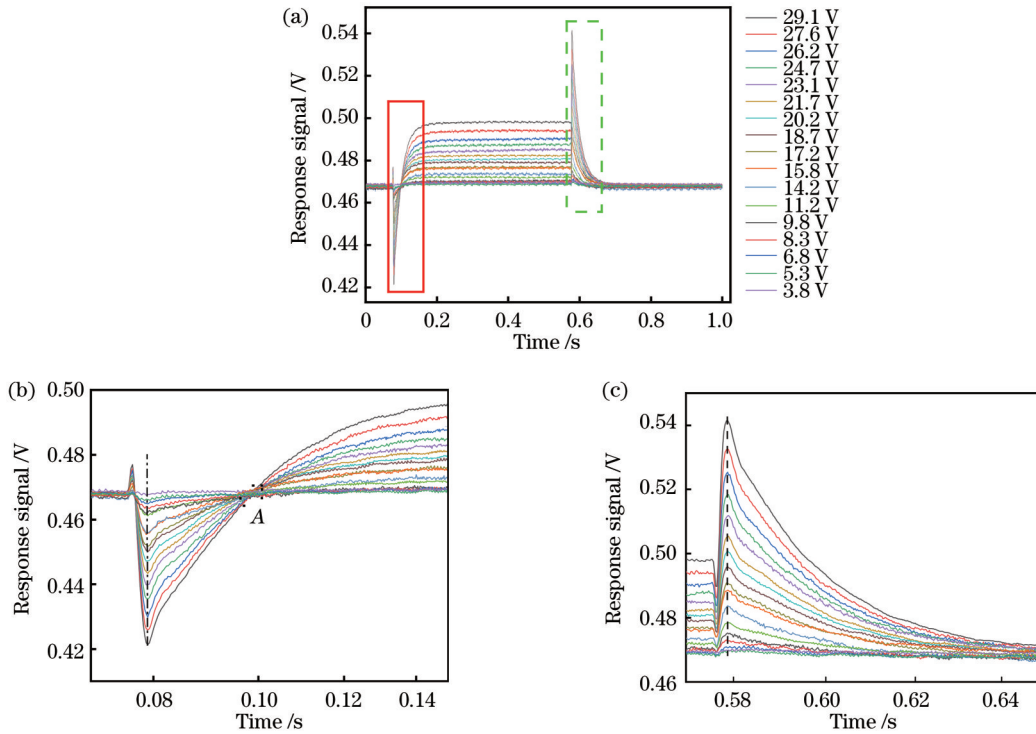


图 4 在不同振幅的正弦电压加载与撤载过程中液体透镜的响应信号。(a) 不同电压驱动下液体透镜的响应信号；(b) 加载电压瞬间不同电压驱动下的液体透镜响应信号；(c) 撤去电压瞬间不同电压驱动下的液体透镜响应信号
 Fig. 4 Response signals of liquid lens during loading and unloading of sinusoidal voltage with different amplitudes. (a) Response signals of liquid lens driven by different voltages; (b) response signals of liquid lens driven by different voltages at the moment of loading voltage; (c) response signals of liquid lens driven by different voltages at the moment of removing voltage

动幅度较大,这一阶段为反冲阶段;随后液体透镜从反冲的峰值位置向目标稳态缓慢变化,即进入正常阶段。由图 4(b)可知,在不同幅度电压的驱动下,它们的响应曲线都交于同一点 A,这一现象将在 3.4 节进行具体分析。

结合图 3,本文进行以下定义:加载时反冲变化量 ΔU_{ur} 为响应信号从 U_0 变化至 U_{um} ,即 $\Delta U_{ur}=U_{um}-U_0$;撤载时反冲变化量 ΔU_{ur} 为响应信号从 U_r 变化至 U_{um} ,即 $\Delta U_{ur}=U_{um}-U_r$;从未加电压驱动时响应信号的稳定值 U_0 至加电压驱动响应信号稳定值 U_r 的变化量为 $\Delta U=U_r-U_0$ 。

图 5 所示为加载过程和撤载过程中反冲变化量与输入电压振幅的关系。图 5(a)中实心方框曲线与实心圆圈曲线分别表示不同驱动电压下的 ΔU_{ur} 和 ΔU_{ur} ,可以看到,无论是加载过程还是撤载过程,反冲幅度绝对值均随驱动电压的增加而增大,对于同一驱动电压,加载过程的反冲幅度绝对值小于撤载过程反冲幅度的绝对值。图 5(b)所示为加载驱动响应信号的变化幅度与加载电压大小的关系,可以看到, ΔU 随加载电压的增加而增大。图 5(c)所示为不同输入电压下加载与撤载的反冲幅度和加载时输出信号变化幅度之比与

加载电压的关系,实心方框与实心圆圈曲线分别表示不同驱动电压下的 $\Delta U_{ur}/\Delta U$ 和 $\Delta U_{ur}/\Delta U$ 与加载电压的关系。由图 5(c)可知,在实验误差范围内 $\Delta U_{ur}/\Delta U$ 与 $\Delta U_{ur}/\Delta U$ 几乎不随驱动电压的大小而变化,近似为一常数。图 5(c)中对应的水平虚线分别为 $\Delta U_{ur}/\Delta U$ 和 $\Delta U_{ur}/\Delta U$ 以 $y=c_1$ 按最小二乘法拟合所得; c_1 分别为 2.5 和 -1.6,表明反冲幅度均大于加载时响应信号的变化幅度,而加载反冲幅度大于撤载反冲幅度。

在图 5(d)中,倒三角曲线表示加载时整体响应时间 ΔT_1 ,空心圆圈曲线表示撤载时整体响应时间 ΔT_2 ,五角星曲线表示加载时的反冲响应时间 Δt_1 ,菱形曲线表示撤载时反冲响应时间 Δt_2 。由图 5(d)可知:在实验误差范围内 ΔT_1 、 ΔT_2 、 Δt_1 及 Δt_2 均不随驱动电压变化;4 条水平直线分别为 ΔT_1 、 ΔT_2 、 Δt_1 和 Δt_2 以 $y=c_2$ 根据最小二乘法拟合的结果, c_2 分别为 76.65、75.62、8.01、8.03 ms。由此可见,在实验误差范围内,加载和撤载过程的反冲持续时间相等,整体响应时间相等,且均与驱动电压的大小无关。

综上所述,所有的实验结果与所提出的理论分析结果一致。

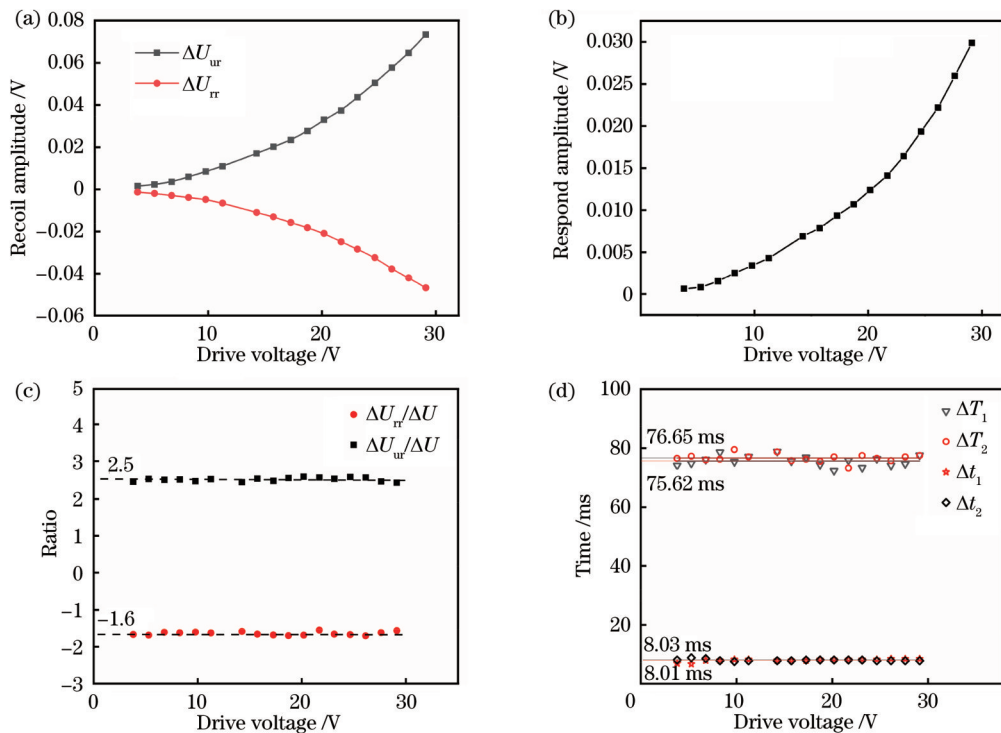


图 5 电压加载过程和撤载过程反冲幅度与输入电压振幅的关系。(a) ΔU_{ur} 和 ΔU_{ur} 与驱动电压幅值的关系; (b) ΔU 与驱动电压幅值的关系; (c) $\Delta U_{ur}/\Delta U$ 和 $\Delta U_{ur}/\Delta U$ 与驱动电压幅值的关系; (d) ΔT_1 、 ΔT_2 、 Δt_1 和 Δt_2 与驱动电压幅值的关系

Fig. 5 Relationship between recoil amplitude and input voltage amplitude during voltage loading and unloading. (a) Relationship between ΔU_{ur} and ΔU_{ur} and driving voltage amplitude; (b) relationship between ΔU and driving voltage amplitude; (c) relationship between $\Delta U_{ur}/\Delta U$ and $\Delta U_{ur}/\Delta U$ and driving voltage amplitude; (d) relationship between ΔT_1 , ΔT_2 , Δt_1 , and Δt_2 and driving voltage amplitude

3.4 暂态过程的测试结果分析

下面分析图 4(b)中为什么不同电压作用下液体

透镜的响应信号交于同一点 A。结合图 3(b), 加载时正常阶段液体透镜响应信号的变化量 ΔU_r 为

$$\Delta U_r = U_r - U_{rm} = U_r - U_0 + U_0 - U_{rm} = \Delta U - \Delta U_{r0} \quad (1)$$

根据图 5(c) 可设

$$\Delta U_r = -k\Delta U, \quad (2)$$

结合式(1)可得

$$\Delta U_r = (1+k)\Delta U. \quad (3)$$

由图 4(b) 可知, A 点的纵坐标为未加驱动电压时的响应信号值 U_0 , 故响应信号从反冲峰值 U_{rm} 变化至 U_0 , 其输出信号的变化量 $\Delta U'$ 为

$$\Delta U' = U_0 - U_{rm} = -\Delta U_{r0}. \quad (4)$$

则结合式(2)~(4), 可得

$$\frac{\Delta U'}{\Delta U_r} = \frac{k\Delta U}{(1+k)} = \frac{k}{1+k}. \quad (5)$$

因为式(5)中 k 为常数, 与所加电压值的大小无关, 故从响应信号反冲峰值 U_{rm} 变化至 U_0 的变化量 $\Delta U'$ 与从 U_{rm} 至 U_r 的总变化量 ΔU_r 的比值与所加电压无关, 而不同驱动电压下响应信号的变化规律相同, 在不同驱动电压作用下, 响应信号从 U_{rm} 变化至 U_0 所需的时间相同, 因此不同电压驱动时的响应信号相交于同一点 A。可见相交于同一点 A 这一实验结果进一步验证了所提出的液体透镜暂态过程理论分析结果的正确性。

4 结 论

电润湿液体透镜响应包括固有响应和强制响应, 其暂态过程的变化规律取决于固有响应, 与驱动电压无关, 这一结果丰富了电润湿液体透镜的相关理论, 对其应用有直接的指导作用; 观察到电润湿液体透镜的反冲现象, 这一发现为合理利用或避免该现象提供了方向, 给出了电润湿液体透镜的设计与制备中需考虑的新的因素, 有助于丰富和完善电润湿液体透镜的工作机理。

参 考 文 献

- [1] Brabcova Z, McHale G, Wells G G, et al. Electric field induced reversible spreading of droplets into films on lubricant impregnated surfaces[J]. Applied Physics Letters, 2017, 110(12): 121603.
- [2] Gao J, Mendel N, Dey R, et al. Contact angle hysteresis and oil film lubrication in electrowetting with two immiscible liquids[J]. Applied Physics Letters, 2018, 112(20): 203703.
- [3] Davoust L, da Cruz C A, Theisen J. On the use of AC electrowetting for biosensing based on dynamic contact angle[J]. Sensors and Actuators B, 2016, 236: 849-857.
- [4] Peykov V, Quinn A, Ralston J. Electrowetting: a model for contact-angle saturation[J]. Colloid and Polymer Science, 2000, 278(8): 789-793.
- [5] Klarman D, Andelman D, Urbakh M. A model of electrowetting, reversed electrowetting, and contact angle saturation[J]. Langmuir, 2011, 27(10): 6031-6041.
- [6] Beni G, Hackwood S, Jackel J L. Continuous electrowetting effect[J]. Applied Physics Letters, 1982, 40(10): 912-914.
- [7] Hayes R A, Feenstra B J. Video-speed electronic paper based on electrowetting[J]. Nature, 2003, 425(6956): 383-385.
- [8] Mishra K, Murade C, Carreel B, et al. Optofluidic lens with tunable focal length and asphericity[J]. Scientific Reports, 2014, 4: 6378.
- [9] Högnadóttir S, Kristinsson K, Thormar H G, et al. Increased droplet coalescence using electrowetting on dielectric (EWOD) [J]. Applied Physics Letters, 2020, 116(7): 073702.
- [10] Lu G, Hu H, Duan Y Y, et al. Wetting kinetics of water nanodroplet containing non-surfactant nanoparticles: a molecular dynamics study[J]. Applied Physics Letters, 2013, 103(25): 253104.
- [11] Theodorakis P E, Müller E A, Craster R V, et al. Superspreading: mechanisms and molecular design[J]. Langmuir, 2015, 31(8): 2304-2309.
- [12] Wang C, Nam S W, Cotte J M, et al. Wafer-scale integration of sacrificial nanofluidic chips for detecting and manipulating single DNA molecules[J]. Nature Communications, 2017, 8: 14243.
- [13] Chiu C P, Chiang T J, Chen J K, et al. Liquid lenses and driving mechanisms: a review[J]. Journal of Adhesion Science and Technology, 2012, 26(12/13/14/15/16/17): 1773-1788.
- [14] Schuhladen S, Banerjee K, Stürmer M, et al. Variable optofluidic slit aperture[J]. Light: Science & Applications, 2016, 5(1): e16005.
- [15] Berge B, Peseux J. Variable focal lens controlled by an external voltage: an application of electrowetting[J]. The European Physical Journal E, 2000, 3(2): 159-163.
- [16] Kuiper S, Hendriks B H W. Variable-focus liquid lens for miniature cameras[J]. Applied Physics Letters, 2004, 85(7): 1128-1130.
- [17] 席崇宾, 黄荣, 周健, 等. 基于液体透镜的激光多普勒信号品质因子增强技术[J]. 中国激光, 2021, 48(7): 0704003.
- [18] Xi C B, Huang R, Zhou J, et al. Quality factor enhancement technology of laser Doppler signal based on liquid lens[J]. Chinese Journal of Lasers, 2021, 48(7): 0704003.
- [18] 谢娜, 张宁, 赵瑞, 等. 交流作用下电润湿液体透镜动态过程的测试与分析[J]. 物理学报, 2016, 65(22): 224202.
- [18] Xie N, Zhang N, Zhao R, et al. Test and analysis of the dynamic procedure for electrowetting-based liquid lens under alternating current voltage[J]. Acta Physica Sinica, 2016, 65(22): 224202.
- [19] Hu X D, Zhang S G, Liu Y, et al. Electrowetting based infrared lens using ionic liquids[J]. Applied Physics Letters, 2011, 99(21): 213505.
- [20] Choi H, Won Y H. Fluidic lens of floating water using intermediate hydrophilic layer based on electrowetting[J]. IEEE Photonics Technology Letters, 2013, 25(18): 1829-1831.
- [21] Li L Y, Yuan R Y, Wang J H, et al. Optofluidic lens based on electrowetting liquid piston[J]. Scientific Reports, 2019, 9: 13062.
- [22] Sim J H, Kim J, Kim C, et al. Novel biconvex structure electrowetting liquid lenticular lens for 2D/3D convertible display [J]. Scientific Reports, 2018, 8: 15416.
- [23] Liu S, Hua H. Extended depth-of-field microscopic imaging with a variable focus microscope objective[J]. Optics Express, 2011, 19(1): 353-362.
- [24] Kong M M, Chen D, Chen X, et al. Research of the human eye model with variable-focus liquid lens[J]. Microfluidics and Nanofluidics, 2017, 21(3): 40.
- [25] Park I S, Park Y, Oh S H, et al. Multifunctional liquid lens for variable focus and zoom[J]. Sensors and Actuators A, 2018, 273: 317-323.
- [26] 赵瑞, 陈露楠, 孔梅梅, 等. 用于波前补偿的三液体透镜阵列的设计分析[J]. 激光与光电子学进展, 2020, 57(21): 212202.
- [26] Zhao R, Chen L N, Kong M M, et al. Performance analysis of wave-front correction using array based on triple liquid lens[J]. Laser & Optoelectronics Progress, 2020, 57(21): 212202.
- [27] López C A, Hirs A H. Fast focusing using a pinned-contact

- oscillating liquid lens[J]. *Nature Photonics*, 2008, 2(10): 610-613.
- [28] Oku H, Ishikawa M. High-speed liquid lens with 2-ms response and 80.3-nm root-mean-square wavefront error[J]. *Applied Physics Letters*, 2009, 94(22): 221108.
- [29] Chae J B, Hong J, Lee S J, et al. Enhancement of response speed of viscous fluids using overdrive voltage[J]. *Sensors and Actuators B*, 2015, 209: 56-60.
- [30] Hong J, Kim Y K, Kang K H, et al. Spreading dynamics and oil film entrapment of sessile drops submerged in oil driven by DC electrowetting[J]. *Sensors and Actuators B*, 2014, 196: 292-297.
- [31] Hao C L, Liu Y H, Chen X M, et al. Electrowetting on liquid-infused film (EWOLF): complete reversibility and controlled droplet oscillation suppression for fast optical imaging[J]. *Scientific Reports*, 2014, 4: 6846.
- [32] Hong J, Kim Y K, Kang K H, et al. Effects of drop viscosity on oscillation dynamics induced by AC electrowetting[J]. *Sensors and Actuators B*, 2014, 190: 48-54.
- [33] 王飞, 何枫. 微管道内两相流数值算法及在电浸润液滴控制中的应用[J]. *物理学报*, 2006, 55(3): 1005-1010.
- Wang F, He F. A numerical method for two-phase flow in micro channels and its application to droplet control by electrowetting on dielectric[J]. *Acta Physica Sinica*, 2006, 55(3): 1005-1010.
- [34] 赵瑞, 华晓刚, 田志强, 等. 电润湿双液体变焦透镜[J]. *光学精密工程*, 2014, 22(10): 2592-2597.
- Zhao R, Hua X G, Tian Z Q, et al. Electrowetting-based variable-focus double-liquid lens[J]. *Optics and Precision Engineering*, 2014, 22(10): 2592-2597.
- [35] 徐荣青, 孔梅梅, 张宏超, 等. 减少电润湿液体透镜变焦时间的实验研究[J]. *光学学报*, 2020, 40(13): 1322003.
- Xu R Q, Kong M M, Zhang H C, et al. Experimental research on reducing zoom time of electrowetting liquid lenses[J]. *Acta Optica Sinica*, 2020, 40(13): 1322003.

Measurement and Analysis of Transient Process of Electrowetting Liquid Lens

Xu Rongqing¹, Li Lei¹, Kong Meimei^{1*}, Zhang Hongchao²

¹*School of Electronic and Optical Engineering, Nanjing University of Posts and Telecommunications, Nanjing 210023, Jiangsu, China;*

²*Faculty of Science, Nanjing University of Science and Technology, Nanjing 210094, Jiangsu, China*

Abstract

Objective The focal length of the variable-focus optical system can be quickly changed within a certain range, so as to realize the clear imaging of the same objects at different positions or levels, and its function is beyond that of the fixed-focus system. The traditional variable-focus system has a mechanical movement, which restricts its application range. In order to realize zoom without mechanical movement, the variable-focus lens is the key, and an electrowetting liquid lens is an electrically controlled variable-focus lens with excellent performance.

At present, many researchers both in China and abroad have conducted a lot of in-depth research on the mechanism, performance, and application of electrowetting liquid lenses. However, due to the diversity of specific lenses and the complexity of the problems, the theory of electrowetting needs to be perfected, the performance needs to be improved, and new applications need to be developed. In terms of application, the performance of the liquid lens is the key. The two most important performance indexes of the variable-focus lens are the focal length and zoom time after zooming, which depend on the response characteristics of the electrowetting liquid lens. From the transient state to the steady state, the focal length after zooming is determined by the steady-state value, and the response time is determined by the transient process. Whether in theory or the experiment, the research on steady-state responses is much less difficult than that on the transient process, so the current research on the response characteristics of electrowetting liquid lenses mainly focuses on the steady-state response, while the research on the transient process is rarely reported. As a result, there is not a completely clear and unified understanding of the transient process. In this paper, the transient process of electrowetting liquid lenses is measured and analyzed, which is helpful to perfect and enrich the electrowetting theory and expand new applications.

Methods A measurement system of the zoom process of electrowetting liquid lenses is designed and built (Fig. 1). The change process of the output voltage measured by the photoelectric detector with time reflects the zoom process of the liquid lens and indicates the change in the interface state of the liquid lens with time, that is, the response characteristics of the liquid lens. The response processes of an ARCTIC liquid lens (A-25H) under different driving voltages, including the response process of loading and unloading voltage, are measured by the self-designed system. According to the response process, the response times of loading and unloading under different driving voltages are obtained, and the measured results under various conditions are analyzed.

Results and Discussions In this paper, it is proposed that the response of a variable-focus liquid lens driven by voltage includes inherent response and forced response. The functional form of the inherent response signal is determined by various parameters of the liquid lens, and it is not related to the driving voltage. However, its coefficient is related to the driving voltage. The forced response has the same functional form as the driving voltage. The change law of the transient process of liquid lenses depends on the inherent response and is independent of the driving voltage. Therefore, changing the driving voltage for the same liquid lens only changes the amplitude of the transient process response but does not change the changing law of the transient process, and thus the response time of the liquid lens is not affected. The experiment verifies that the response of liquid lenses can be decomposed into inherent response and forced response (Fig. 2). The response process and response time of the liquid lens driven by different voltages are measured [Fig. 5(d)]. It is found that the measured results are consistent with the theoretical analysis results. Moreover, the experimental result that the response signals of the liquid lens intersect at the same point *A* under different driving voltages [Fig. 4(b)] is analyzed, which further verifies the theoretical analysis of the proposed transient process of the liquid lens. In addition, the recoil phenomenon of electrowetting liquid lenses is observed. This phenomenon occurs in the initial stage of loading voltage and unloading voltage.

Conclusions In this paper, it is proposed that the response of electrowetting liquid lenses includes inherent response and forced response, and the changing law of the transient process depends on the inherent response and is independent of the driving voltage. Therefore, the response time of electrowetting liquid lenses is independent of the driving voltage. This conclusion enriches the related theory of electrowetting liquid lenses and has direct guidance for its application. The recoil phenomenon of the electrowetting liquid lens is observed. This finding makes it possible to reasonably utilize or avoid this phenomenon and gives new factors to be considered in the design and preparation of electrowetting liquid lenses, which is helpful to enrich and perfect the working mechanism of electrowetting liquid lenses.

Key words optical devices; active or adaptive optics; liquid lens; transient process; recoil phenomenon